
Since January 2020 Elsevier has created a COVID-19 resource centre with free information in English and Mandarin on the novel coronavirus COVID-19. The COVID-19 resource centre is hosted on Elsevier Connect, the company's public news and information website.

Informatics in Medicine Unlocked 26 (2021) 100755

Contents lists available at ScienceDirect

Informatics in Medicine Unlocked

journal homepage: www.elsevier.com/locate/imu

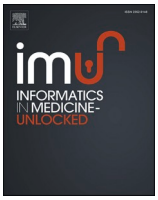

# In-silico study on perovskites application in capturing and distorting coronavirus

ARTICLE INFO

*Keywords*
Nano-perovskite
Molecular dynamics
SARS-CoV-2
COVID-19
ACE2
Spike protein

ABSTRACT

The COVID-19 pandemic, known as coronavirus pandemic, a global pandemic, emerged from the beginning of 2020 and became dominant in many countries. As COVID-19 is one of the deadliest pandemics in history and has a high rate of distribution, a fast and extensive reaction was needed. Considering its composition, revealing the infection mechanism is beneficial for effective decisions against the spread and attack of COVID-19. Investigating data from numerous studies confirms that the penetration of SARS-CoV-2 occurs along with bonding spike protein (S protein) and through ACE2; Therefore, these two parts were the focus of research on the suppression and control of the infection. Performing lab research on all promising candidates requires years of experimental study, which is time-consuming and not an acceptable solution. Molecular dynamic simulation can decipher the performance of nano-structures in preventing the spread of coronavirus in a shorter time. This study surveyed the effect of three nano-perovskite structures ($SrTiO_3$, $CaTiO_3$, and $BaTiO_3$), a cutting-edge group of perovskite materials with outstanding properties on coronavirus. Various computational parameters evaluate the effectiveness of these structures. Results of the simulation indicated that $SrTiO_3$ performs better in SARS-CoV-2 suppression.

## 1. Introduction

COVID-19 is a widespread disease that primarily affects the respiratory system and is caused by SARS-CoV-2, or β-coronavirus [1] spread abruptly from December 2019. From the first case report in December 2019 in Wuhan, Hubei Province, China, it took less than a month that the reported case in China reached 41 patients on January 2, 2020 and 571 issues on January 22, 2020 in China and soon after 5th April the reported instances of COVID-19 pandemic crossed 311,000 [2]. More than millions of people around the world are affected by COVID-19, and the range of their infections are varied from mild respiratory symptoms to acute respiratory distress syndrome (ARDS) and even death. The virus transforms by human-to-human contact through inhalation of infected droplets and contact with contaminated surfaces. The most common symptoms include fatigue, headache, fever, and cough [3].

Numerous attempts have been made to profoundly visualize and understand the complicated biological structure of the SARS-CoV-2 structure. In January 2020, the genome sequence of SARS-CoV-2 was realized, which led to identifying infection mechanisms. The genome decoding shows that twenty different proteins can be found in the SARS-CoV-2 structure, categorized into four main groups of S: Spike, E: Envelope, M: Membrane, and N: Nucleocapsid [1]. The fusion of the SARS-CoV-2 into the body occurs by the binding of cellular receptors. Spike glycoprotein, a trimeric protein, binds with the cell through angiotensin-converting enzyme 2 (ACE2) [4]. ACE2 is smaller and interacts with various human tissues, including lung, liver, stomach, ileum, kidney, and colon [5,6]. Full-length ACE2 combines the N-terminal peptidase domain (PD) and C-terminal-like collection-like domain (CLD) that has helix as transmembrane and 40-residue intercellular segment. In most studies, due to the complexity of the CLDs, only PD is considered in the calculations and simulations [4].

Furthermore, studies proved the higher responsibility of PD in SARS-CoV-2 infection compared to CLD [7]. PD, a small protein domain of the ACE2 with many functional groups, has a solid affinity to bind with other molecules, including COVID-19 [8]. For viral endocytosis and propagation, proteolysis of the S1/S2 subunits is essential. S1 subunit is a receptor responsible for binding with PD, and the S2 subunit is related to membrane fusion [9,10]. In other words, after ACE 2 binds S1 with a dissociation constant of approximately 15nM, S2 exposes via the cleavage sitting. Thus, it is crucial in viral infection. Moreover, transmembrane protease serine 2 (TMPRSS2) (which is responsible for the entry of influenza A and other types of coronavirus), Basigin (CD147), Cathepsin B, and Cathepsin L may provide the condition for ACE2 cleavage [3] and SARS-CoV-2 spike protein transmembrane activation [11]. ACE2 simulates the renin-angiotensin system (RAS), a hormone that regulates blood pressure, fluid, and electrolyte balance. This cleavage, in turn, results in the binding of ACE2 receptor and receptor-binding domain (RBD) of spike protein from the virus. In this stage, 5–6 days of incubation usually happens to see the primary symptoms of SARS-CoV-2 [1]. For this, a compelling approach toward COVID-19 inhibition is targeting S protein and ACE2 [10].

In numerous attempts toward COVID-19 vaccine production, three approaches have been inquired, resulting in three types of vaccine production; protein-based vaccine, viral vector vaccine, and nucleic acid vaccine. The protein-based vaccine produced with recombination technique uses the subunits of the viral antigenic parts. Viral vector vaccines seize the protein machinery of host cells. Their main drawback is that they may be ineffective on the people exposed to the virus previously. Nucleic-based vaccines that are broadly used in the United States and Europe work based on the autoimmunity phenomenon, which contains cross-reaction of the S protein and ACE2. The potential drawbacks are related to immune-mediated patients, dose dependency, and age-

https://doi.org/10.1016/j.imu.2021.100755
Received 21 July 2021; Received in revised form 4 October 2021; Accepted 8 October 2021
Available online 10 October 2021

targeting. Thus, the direct approach is focused on spike protein targeting to trigger antibody production in the body. The RNA-based vaccine consists of S protein which is replication-deficient, and the antibody production will become robust. To encounter this nano-virus, taking advantage of an engineered nano-medicine can extend the limits of using an effective therapy [1].

Different nano-structures have been considered for therapeutic approaches. Perovskites provide a positive surface charge for fabulous behavior in aqueous media [12]. Perovskites semiconductors, which can be represented as $A^{3+}B^{3+}O_3$ [2–13], show spectacular properties in different fields of science. The applications include solar cells [14], portable and wearable electronic devices [15], nuclear radiation of monitoring [16], membranes [17], and recently in medicine such as photo-medicine and bioelectric implants. In this paper, we considered Perovskites, for the first time, as a suppression agent for COVID-19. For this aim, we applied Molecular Dynamics (MD) simulation, which is an effective method for proposing the most promising materials in this regard. As the animal study is time-consuming and expensive, using the selected combination speeds up the research in circumstances [1]. This study simulated the spike proteins that encounter a specific perovskite structure ($SrTiO_3$, $CaTiO_3$, $BaTiO_3$) before ACE2. To investigate the effect of these perovskite structures on the deactivation of a spike protein, coarse-grained MD simulations have been used (CGMD). Energy, root-mean-square deviation (RMSD), root-mean-square fluctuation (RMSF), solvent accessible surface area (SASA), distribution of secondary structure of prediction (DSSP), number of h-bonds, and the radius of gyration have been investigated in this simulation.

## 2. Method

Classic MD simulation has been constructed on the idea of no bond-forming or breaking where Newton's equation of motion is based on the interaction potential for the periodic behavior of a one-dimensional inharmonic chain (Fermi-Pasta-Ulam) and three-dimensional hard-sphere model (Alder-Wainwright) are applied [18]. In this study, CGMD has been used for the simulation. In this method, small groups of atoms are assumed to be a single unit; thus, larger timescales might be investigated. The equations in CGMD are similar to classical MD. Thus the results are in total agreement with the atomic scale simulation. This method is widely used for polymeric chains materials. Considering specified chemical bonds, including; bending, twisting, and stretching, comprehensive research becomes applicable.

In this work, molecular simulations on all-atom, CGMD, and docking have been performed to examine the interaction between the S protein of Covid-19 and the coarse PD of ACE2. Three simulations consider all-atom and CGMD between S protein and perovskite structures, and the rest, docking simulations of deformed S protein and ACE2. The distorting in the structure of the spike protein can be observed in Fig. 1.

### 2.1. Simulation details

In this study, GROMACS software was used for both MD simulations and data analyses. The energy was calculated using the molecular mechanics Poisson-Boltzmann surface area (MMPBSA) computational package. Modelling the structures has been done with a system of 32-core X5670 CPU with 1080 Ti graphics card and an Ubuntu 18.04.1 operating system. The CGMD simulation with the Martini force field has been used, and Umbrella sampling with 100 configurations at 3000ns with time steps of 30 fs were performed, using the cut-off radius of 3 nm. The spike protein structure and ACE2 were downloaded from the RSCB website, both with the pdb ID of 6M0J, and the perovskite structures were designed via Avogadro software, and the most stable state was reached using Gaussian software. DFT (b3lyp) was the optimization method with a basic set of 6–31++G. Also, in the topology file, the electrostatic potential (ESP) charges were calculated and imported. For topography data on spike protein, the Computed Atlas of Surface Topography of Proteins (CASTP) server has been used [19]. The gmx editconf, gmx insert molecules and gmx solvate commands. Avogadro software was used to design the dimensions of the box and add the molecules and the solvent (the solvent is water to represent aqueous media [20]). The pH of the media was assumed to be 7.0 in the NTP and NVP simulation. Moreover, the temperature of 300K and the pressure of 1 bar were implemented in this simulation.

### 2.2. Molecular docking

AutoDock_vina_1_1_2_linux_x86 was used for docking in this simulation [21]. The center of the box is placed at x = −11.57, y = −5.22 and

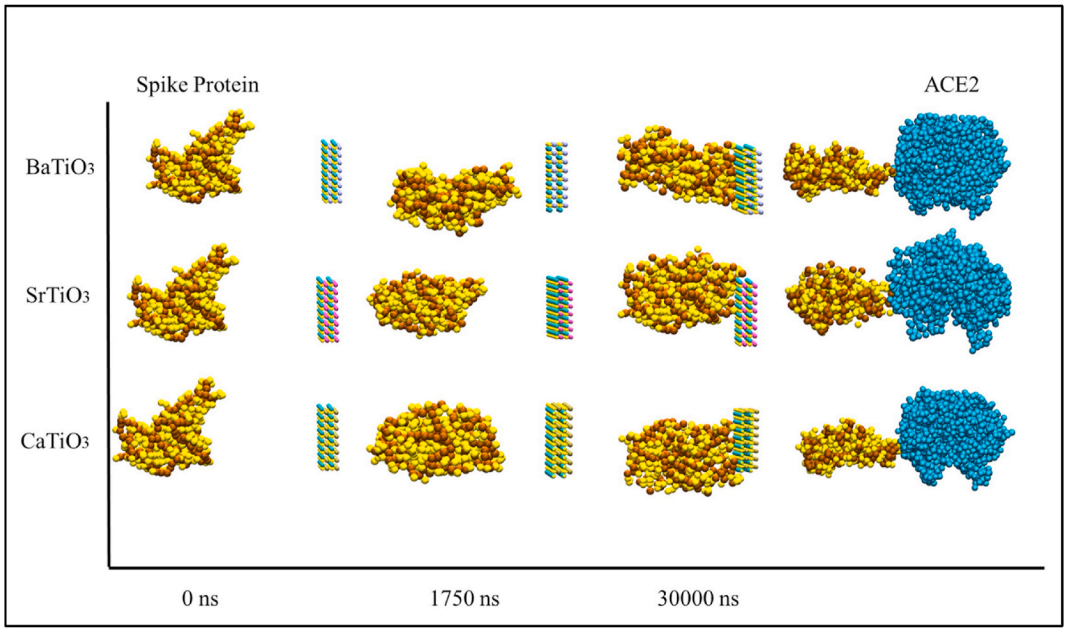


**Fig. 1.** The process of encountering the spike protein with $BaTiO_3$, $CaTiO_3$, and $SrTiO_3$ nanostructure in 0ns, 1750ns and 3000 ns. The distorted spike protein then collides with the ACE2.

z = 11.67 and the box length was x = 32, y = 32 and z = 42 Å. The gasteiger charge and polar hydrogen were added using the AutoDock Tool-1.5.6 to the SARS-CoV-2 RBD pdb and ACE2 pdb file, respectively.

## 3. Results

### 3.1. Energy

The intermolecular interaction energy indicates the nanostructure's power to distort or deform the spike protein [22,23]. The aim is to restrain the S protein from penetrating through the ACE2 cell channel. Therefore, the energy between the considered nanostructures with spike protein has been calculated. As shown in Fig. 2, both van der Waals (VdW) and the S protein's electrostatic energy levels in the presence of $BaTiO_3$, $CaTiO_3$, and $SrTiO_3$ nanostructures have been reduced. The presence of nanostructures increases the interactions energies. A negative sign indicates that the energy interactions are of the attraction type and not repulsive. This fact infers that using a nano-perovskite structure benefits us by decreasing the probability of successful collision; however, using the proper combination is helpful to improve the performance and take complete advantage of this structure. In other words, after exposing the S protein to nano-perovskite structures, the absolute value of energy for re-docking of S protein and PD from ACE2 decreased significantly for all of the structures. This is more obvious for $SrTiO_3$, which proves the distortion and deformation in the S protein structure. It decreases the active site for the interaction and consequently decreases the probability of infection by COVID-19. In this work, different analyzes have been used. Table 1 contains the average of the most important molecular analyzes, which are explained in detail by the rest of the figures.

### 3.2. Radius of gyration

The radius of gyration explains the compactness of the structure as a function of time, which can be used in analyzing the quality of bonds, whether they are weak or tight. Fig. 3 shows the results of the radius of gyration study in the presence of $BaTiO_3$, $CaTiO_3$, and $SrTiO_3$ nanostructures to decrease the radius of gyration by contacting three nano-perovskite structures. Fig. 3 reveals that at the start of the simulation, all the nano-perovskite effects on the compactness. As a result, the S protein and ACE2 bonding are neglectable. Afterward, the structures' compactness fluctuates (in the presence of all perovskite structures) in a limited range. From 2000,000 ps onward, the effect of spike protein on $SrTiO_3$ compactness is more vibrant. Less falling in the compactness of the structure is more favorable in the adsorption of spike protein on this perovskite structure.

**Table 1**
The total energy, Rg and average SASA of the spike protein encountered both ACE2 and perovskite nanostructures.

| Total Energy (KJ/mol) | | |
|---|---|---|
| | Energy with nanostructure | Energy with ACE2 |
| **$BaTiO_3$** | −150.613 | −273.546 |
| **$CaTiO_3$** | −121.647 | −289.655 |
| **$SrTiO_3$** | −95.974 | −301.831 |
| **Rg(ns)** | | |
| **$BaTiO_3$** | 1.30072395 | |
| **$CaTiO_3$** | 0.447702967 | |
| **$SrTiO_3$** | 0.12459869 | |
| **Average of SASA (nm [2]** | | |
| **$BaTiO_3$** | 204.919495 | |
| **$CaTiO_3$** | 206.55445 | |
| **$SrTiO_3$** | 208.969104 | |

### 3.3. RMSD and RMSF

RMSD implies the flexibility of an atom to depart the S protein. Fig. 4. a shows the average distance between a specific spike protein and ACE2 in the presence and absence of perovskite nanostructure. According to Fig. 4. a, the average RMSD value between the S protein and ACE2 is higher than the S protein and ACE2 in the presence of perovskite nanostructure. The higher the RMSD value, the more flexibility in the particle's movements due to thermal fluctuations.

RMSF is the displacement in a single atom or a molecular structure of a reference atom or structure. Fig. 4. b infers the RMSF value for the studied perovskite structures. The highest residue implies loosely bonds such as bend, turn, and coil that make the whole complex unstable and decrease the probability of S protein's diffusion via ACE2. As shown in Fig. 4. b, $SrTiO_3$ perovskite nanostructure causes the RMSF level to increase from 3.347nm to 8.185nm. Despite $SrTiO_3$, $BaTiO_3$ decreases this value from 8.134 nm to 3.546 nm, increasing viral penetration in the body.

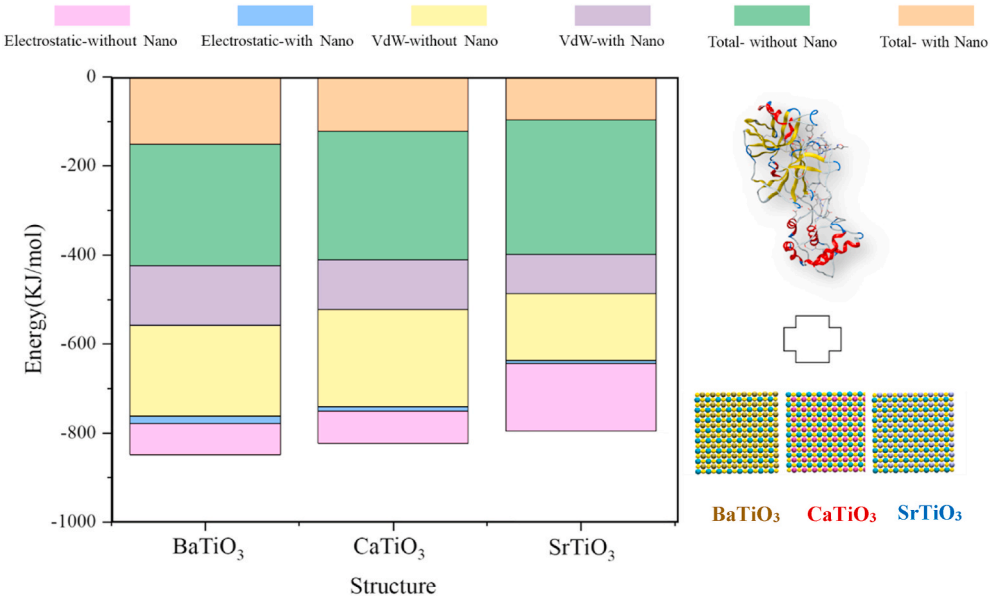


**Fig. 2.** Electrostatic and van der Waals energy levels for Spike protein in direct contact with ACE2 and in the presence of $BaTiO_3$, $CaTiO_3$, and $SrTiO_3$ nanostructures.

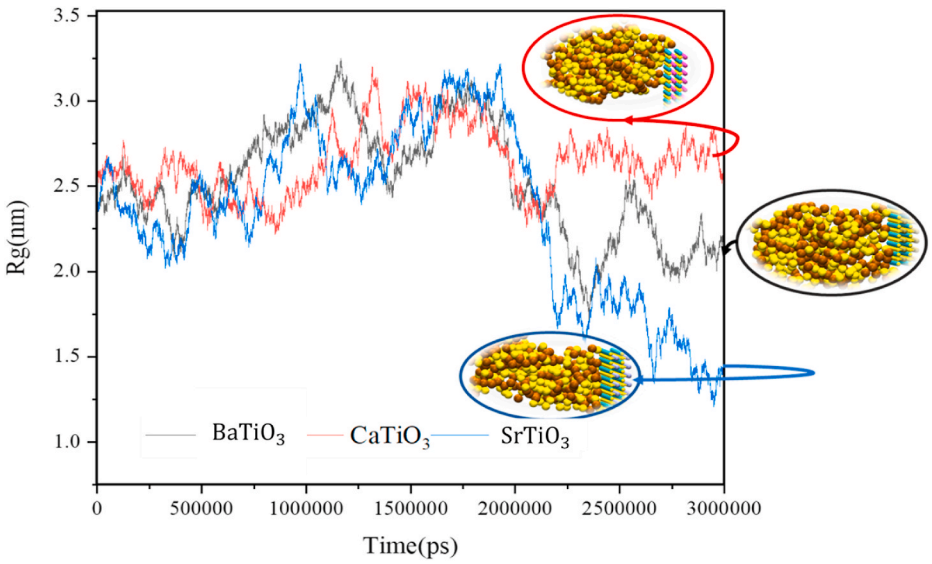


**Fig. 3.** The radius of gyration for $BaTiO_3$, $CaTiO_3$, and $SrTiO_3$ encountering spike protein.

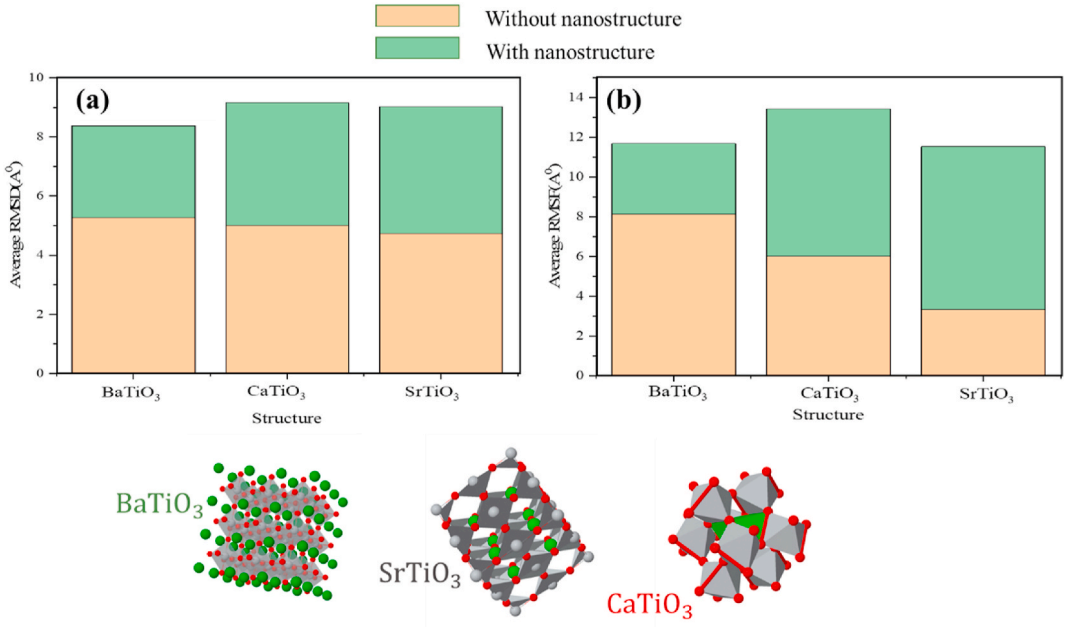


**Fig. 4.** a. RMSD and b. RMSF for spike protein with and without $BaTiO_3$, $CaTiO_3$, and $SrTiO_3$ nanostructures.

### 3.4. SASA

The capacity of a material in an aqueous media to be surrounded by water molecules is defined as SASA [24]. Higher active sites accessible result in higher capacity, which can be calculated via equation (1).

$$\delta G = \sum \delta \sigma_i A_i \tag{1}$$

where σ is the atom *i* solvation parameter, and A is the accessible surface area.

Fig. 5 demonstrates that the SASA value of $SrTiO_3$ is higher at the beginning of the simulation. A deterioration was observed in the SASA for $SrTiO_3$ and an improvement for $CaTiO_3$, while the average SASA for $BaTiO_3$ is constant despite all of the fluctuations. Higher SASA for the S protein leads to a higher chance of penetration in the cell from the ACE2 channel in the body fluid medium.

### 3.5. Number of H-bonds

The number of H-bonds is whenever an electron donners and an electron acceptor gradually interact through a non-binding reaction in the electrostatic interaction. Fig. 6 shows the number of intermolecular hydrogen bonds for the investigated structures. In the absence of the perovskite nanostructures, hydrogen bonds are around 40, while Nano-perovskite reduces this value.

### 3.6. Distribution of secondary structure (DSS)

Configuration changes in the SP after contacting with nano-perovskite have been shown in Fig. 6. As mentioned, increasing the coil, bend, and turn and decreasing the β-sheets and α-helices helps reduce the S protein's stability. As illustrated in Fig. 7, all the studied perovskites reduce the S protein's stability. SrTiO3 is beneficial as it

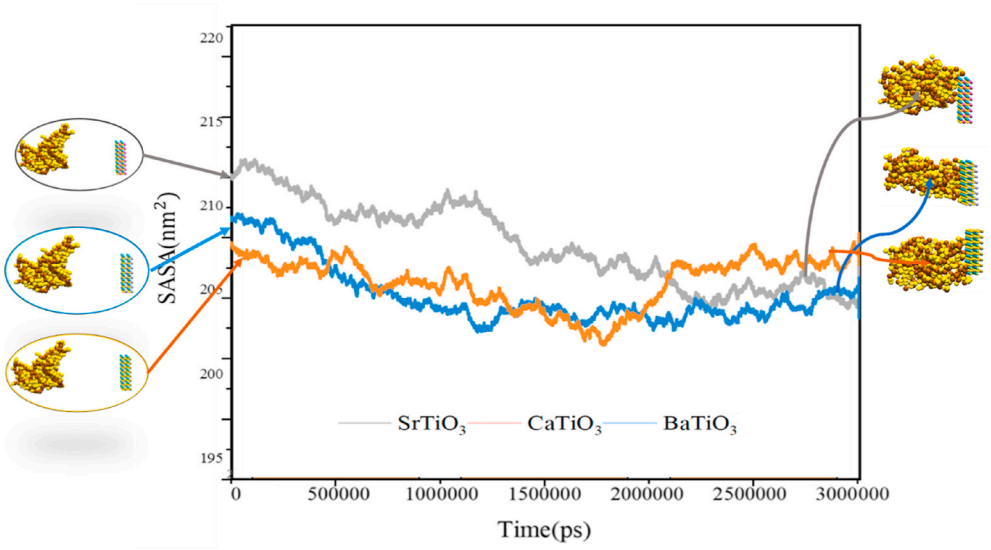


**Fig. 5.** SASA of $BaTiO_3$, $CaTiO_3$, and $SrTiO_3$ for adsorption of the spike protein.

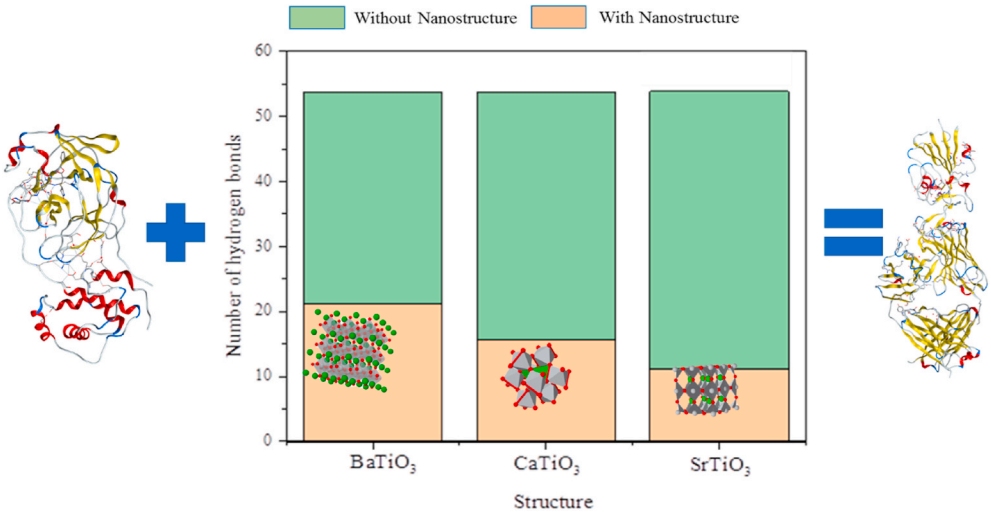


**Fig. 6.** The number of hydrogen bonds between spike protein and ACE2 in the presence and absence of $BaTiO_3$, $CaTiO_3$, and $SrTiO_3$ nanostructures.

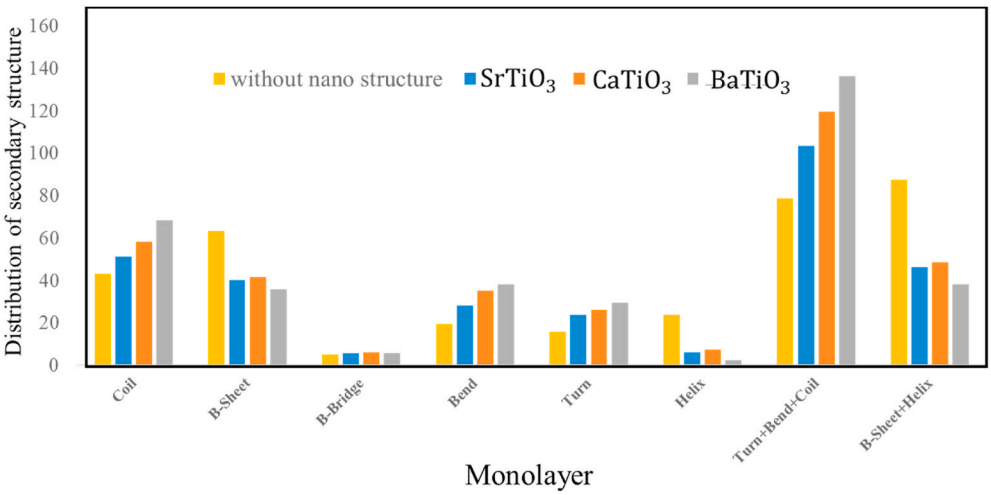


**Fig. 7.** Distribution of secondary structures for S protein without and with $BaTiO_3$, $CaTiO_3$, and $SrTiO_3$ nanostructures.

increases coil, bend, and turn from 45.98% to 66.57% and reduces the β-sheets and α-helices from 51.02% to 29.88%. The process of the helix, β-sheet and β-sheet-helix unfolding was accompanied by the number of H-bonds reduction [25]. This also causes an increase in the number of interpeptide contacts and random un-oriented coil formation. Moreover, 4–5 amino acids and internal hydrogen bonds encourage the turn increment [26]. As a result, while the number of β-sheet and helix decreases, the number of coil and turns increases.

## 4. Discussion

The energy diagram reveals that, although all of the three studied perovskite structures effectively decrease the energy level, $SrTiO_3$ plays the best role in this era, reducing VdW and electrostatic energy levels significantly from −150.231 and −151.6 to −88.946, −7.028 KJ/mol. Moreover, based on the radius of gyration, $SrTiO_3$ with an average level of 0.12459869 nm is the best nano-perovskite structure. In addition, our finding on the RMSD and RMSF confirms that using a perovskite can limit the flexibility of the structure, which is not desirable. Nevertheless, $SrTiO_3$ decreases the flexibility of the structure more slightly from 4.735 nm to 4.294 nm; it is more favorable to use as a means to control the penetration of SARS-CoV-2 through ACE2 in the cells. Furthermore, Fig. 5 indicated that decreasing the SASA levels by applying different perovskite is desirable, and nano-$SrTiO_3$ is the best for controlling the diffusion of S protein. Last but not least, nano-$SrTiO_3$ perovskite decreases the number of hydrogen bonds more significantly than other nano-structure, which shows that the fewer covalent bonds are responsible for a lower chance of viral infection in the body by using $SrTiO_3$.

## 5. Conclusion

In the study, MD simulations on COVID-19 have been performed to investigate the effect of nano-perovskite structure on suppressing the infection and the probability of distribution of SARS-CoV-2 in the body. In this computational work, the distribution of the virus was studied by investigating the effect of nano-$SrTiO_3$, nano-$BaTiO_3$, and nano-$CaTiO_3$ by various metrics such as Energy, RMSD, RMSF, SASA, Number of H-bonds, and DSS factors. Analyzing the effect of simulated nano-perovskite structures showed that nano-$SrTiO_3$ has the most distinguished effect on suppressing the COVID-19 by distorting and deforming the S protein and, as a result, decreasing the possibility of penetration and viral propagation.

## Funding

The authors declare no competing financial interest.

## Declaration of competing interest

The authors declare that they have no known competing financial interests or personal relationships that could have appeared to influence the work reported in this paper.

## Acknowledgements

The authors wish to acknowledge Ali Mohammadi for his support editing. We would also like to show our appreciation to Sadegh Alavi for sharing in the conceptualization and editing of this work.

## References

[1] Mouffouk C, et al. Eur J Pharmacol 2020;891:173759.
[2] Hamid S, et al. New microbes and new infections. 2020. p. 100679.
[3] Gu SX, et al. Nat Rev Cardiol 2020:1.
[4] Yan R, et al. Science 2020;367(6485):1444.
[5] Mehalko J, et al. Protein expression and purification, vol. 179; 2020. p. 105802.
[6] Khedri, M., et al., (2021).
[7] Perrella F, et al. Biomolecules 2021;11(7):1048.
[8] Sitthiyotha T, Chunsrivirot S. Sci Rep 2021;11(1):1.
[9] Kirchdoerfer RN, et al. Nature 2016;531(7592):118.
[10] Rathod SB, et al. In silico pharmacology 2020;8(1):1.
[11] Poland GA, et al. SARS-CoV-2 vaccine development: current status. In: Mayo clinic proceedings. Elsevier; 2020.
[12] Chauhan G, et al. ACS Nano 2020;14(7):7760.
[13] Jonker G, Van Santen J. Physica 1950;16(3):337.
[14] Hodes G. Science 2013;342(6156):317.
[15] Xu C, et al. Microsystems & Nanoengineering 2021;7(1):1.
[16] Yu D, et al. Nat Commun 2020;11(1):1.
[17] Zhao J, et al. Nat Photonics 2020;14(10):612.
[18] Amati G, Schilling T. Chaos: An Interdisciplinary Journal of Nonlinear Science 2020;30(3):033116.
[19] Helal MA, et al. J Biomol Struct Dyn 2020:1.
[20] Basit A, et al. J Biomol Struct Dyn 2020:1.
[21] Trott O, Olson AJ. J Comput Chem 2010;31(2):455.
[22] Bernshtein V, Oref I. J Chem Phys 1998;108(9):3543.
[23] Xiang B, et al. Science 2020;368(6491):665.
[24] Zhang D, Lazim R. Sci Rep 2017;7(1):44651.
[25] Kabsch W, Sander C. Biopolymers: Original Research on Biomolecules 1983;22 (12):2577.
[26] Qi R, et al. Biomacromolecules 2014;15(1):122.

Mohammad Khedri
*Computational Biology and Chemistry Group (CBCG), Universal Scientific Education and Research Network (USERN), Tehran, Iran*

Pegah Zandi
*School of Metallurgy and Materials Engineering, College of Engineering, University of Tehran, Tehran, Iran*

Ebrahim Ghasemy
*Nanotechnology Department, School of New Technologies, Iran University of Science and Technology, Tehran, Iran*

Arash Nikzad
*Department of Mechanical Engineering, University of British Columbia, 2054-6250 Applied Science Lane, Vancouver, BC V6T1Z4, Canada*

Reza Maleki**
*Computational Biology and Chemistry Group (CBCG), Universal Scientific Education and Research Network (USERN), Tehran, Iran*

Nima Rezaei*
*Research Center for Immunodeficiencies, Pediatrics Center of Excellence, Children's Medical Center, Tehran University of Medical Sciences, Tehran, Iran*
*Network of Immunity in Infection, Malignancy and Autoimmunity (NIIMA), Universal Scientific Education and Research Network (USERN), Tehran, Iran*
*Department of Immunology, School of Medicine, Tehran University of Medical Sciences, Tehran, Iran*

** Corresponding author.

* Corresponding author. Research Center for Immunodeficiencies, Pediatrics Center of Excellence, Children's Medical Center, Tehran University of Medical Sciences, Tehran, Iran.
*E-mail address:* rezamaleki96@gmail.com (R. Maleki). (N. Rezaei)
rezaei_nima@tums.ac.ir (N. Rezaei)